Cytoskeletal Rearrangements and the Functional Role of T-Plastin during Entry of *Shigella flexneri* into HeLa Cells

T. Adam,*‡ M. Arpin,*§ M.-C. Prévost,*‖ P. Gounon,*‖ and P. J. Sansonetti*‡

*Unité de Pathogénie Microbienne Moléculaire and U389 Institute National de la Santé et de la Recherche Médicale,‡ Unité de Biologie des Membranes,§ Station Centrale de Microscopie Electronique,‖ Institut Pasteur, Paris, 75724 Paris Cedex 15, France

Abstract. *Shigella flexneri* is an enteroinvasive bacterium which causes bacillary dysentery in humans. A major feature of its pathogenic potential is the capacity to invade epithelial cells. *Shigella* entry into epithelial cells is considered a parasite-induced internalization process requiring polymerization of actin. Here we describe the cytoskeletal rearrangements during *S. flexneri* invasion of HeLa cells. After an initial contact of the bacterium with the cell surface, distinct nucleation zones of heavy actin polymerization appear in close proximity to the contact site underneath the parasite with long filaments being polymerized. These structures then push cellular protrusions that rise beside the entering bacterium, being sustained by tightly bundled long actin filaments organized in parallel orientation with their positive ends pointing to the cytoplasmic membrane. Finally, the cellular projections coalesce above the bacterial body, leading to its internalization. In addition, we found the actin-bundling protein plastin to be concentrated in these protrusions. Since plastin is known to bundle actin filaments in parallel orientation, colocalization of parallel actin filaments and plastin in the cellular protrusions strongly suggested a functional role of this protein in the architecture of parasite-induced cellular projections. Using transfection experiments, we show the differential recruitment of the two plastin isoforms (T- and L-) into *Shigella* entry zones. By transient expression of a truncated T-plastin which is deprived of one of its actin-binding sites, we also demonstrate the functional role of T-plastin in *Shigella* entry into HeLa cells.

BACTERIAL entry into epithelial cells is likely to trigger a cascade of transmembrane and intracellular signals leading to major cytoskeletal rearrangements (29, 59, 61). The enteroinvasive bacterium *Shigella flexneri* is a gram negative bacillus causing bacillary dysentery in humans. A major step in the pathogenesis of the disease is invasion of colonic epithelial cells (67, 70). Noninvasive mutants of *Shigella* are avirulent (27, 36, 44, 60, 62). The invasive phenotype of *S. flexneri* is conferred by a 37-kb region of a 220-kb virulence plasmid (50, 62). Three of the proteins encoded by this region, IpaB, IpaC, and IpaD have recently been shown to be essential for bacterial entry and for the lysis of the phagocytic vacuole (36, 51). *Shigella* entry is generally considered as a process of parasite-specified endocytosis that mimics phagocytosis with actin polymerization in the eukaryotic cell resulting in the formation of an intracellular vacuole containing the bacterium (7, 32).

In general, cellular uptake of a bacterium is considered to start with the adherence to the host cell. Several epithelial cell receptors which are involved in bacterial entry have been described; for example, different members of the β1 integrin family bind to Invasin, an outer membrane protein that mediates adherence and internalization of enteropathogenic *Yersinia* into epithelial cells (37). The epidermal growth factor receptor (EGFR)[1] has been shown to be implicated in entry of *Salmonella typhimurium* into Henle-407 cells (26).

Adherence of *S. flexneri* to epithelial cells is poor (7). There is no cellular receptor known to promote its adhesion. For bacterial entry, there is an absolute requirement of actin polymerization in the host cell (7). This seems to be a common attribute of enteroinvasive bacteria thus far studied including enteropathogenic *E. coli* (19), *Salmonella* (16), *Yersinia* (15, 35), and *Listeria* (25). In addition, myosin colocalizes with *S. flexneri* entry spots (7). These features resemble phagocytosis performed by professional macrophages (4, 65). However, receptor-mediated endocytosis may also play a significant role during entry of *S. flexneri* into HEp-2 cells since clathrin can be found in bacterial invasion complexes and bacterial penetration of these cells can be inhibited by K^+-depletion, a procedure known to block coated pit formation, a major characteristic of this kind of particle uptake (9, 33). The fact that bacterial internalization

Please address all correspondence to Dr. Philippe J. Sansonetti, Institut Pasteur, Unité de Pathogénie Microbienne Moléculaire, 28, rue du Dr. Roux, 75724 Paris Cedex 15, France. Tel.: 33 1 45 68 8342. Fax: 33 1 45 68 8953.

1. *Abbreviations used in this paper*: EGFR, epidermal growth factor receptor; EPEC, enteropathogenic *E. coli*; rt, room temperature.

can be completely blocked by inhibition of either actin polymerization or coated pit formation (9, 32) may indicate that both of the two types of particle uptake participate in a common entry mechanism rather than represent alternative forms of parasite internalization as described for chlamydia (47, 58). Thus, *Shigella* entry does not seem to follow one of the classical entry pathways like phagocytosis or receptor-mediated endocytosis but rather represents a hybrid of several mechanisms. After lysis of the phagosome, bacteria multiply and move freely, or along actin cables, within the cell and infect adjacent cells via bacterial protrusions (2, 3, 38, 48, 55, 63, 64, 69). Recent evidence indicates that *Salmonella* induces membrane "ruffling" upon entry into epithelial cells (20, 21). There is a possibility that *Shigella*, in a similar manner, induces a macropinocytotic process that achieves entry.

To better characterize this actin-mediated entry process, we are presenting here a detailed morphological description of a sequence of major cytoskeletal rearrangements during *Shigella* entry into HeLa cells. We paid particular attention to the microarchitecture of the cellular protrusions that arise around the intruding bacterium and depicted a number of cellular activities necessary to achieve bacterial internalization. This should help identify molecules that are necessary for bacterial parasitism of eukaryotic cells. Thus, the initial observation that cellular projections surrounding the penetrating bacterium contain very tightly packed F-actin in parallel orientation prompted us to study a possible association of the actin-bundling protein plastin with bacterial invasion. Plastin, an F-actin cross-linking protein, is homologue to fimbrin which was first isolated from chicken intestinal brush borders (5, 6, 13). This protein has been shown to be part of the tail-like structure that forms behind bacteria that move in the cytoplasm or are found in bacterial protrusions during cell-cell spread (57). In addition, a homologue of plastin has been shown to play a functional role in endocytosis in yeast (42). Here we show a succession of major cytoskeletal rearrangements induced by the penetrating bacterium and provide evidence for the functional role of plastin in epithelial cell invasion by *Shigella*.

Materials and Methods

Bacteria

M90T is a wild-type invasive strain of *S. flexneri* serotype 5. BS176 is a noninvasive mutant of M90T cured of the 220-kb virulence plasmid. The plasmid (pIL22) encodes an afimbrial adhesin of uropathogenic *E. coli* (43) that promotes bacterial adherence to human epithelial cells. The strains SC301 and SC300 are M90T or BS176 containing pIL22, respectively, as previously described (7). SC560, an IcsA mutant negative for intercellular spread (2), was used for quantitative entry assays. Enteropathogenic *E. coli* (EPEC) strain E2348 (39) served as a control.

Cells

HeLa cells were routinely grown in 35-mm dishes and 2 ml of minimal essential medium (MEM with glutamine; GIBCO BRL, Gaithersburg, MD) with 10% FCS (GIBCO BRL). 22 × 22 mm coverslips placed in 35-mm dishes were used to grow cells for immunofluorescence studies. For quantiative entry assays, we used tTA-transfected HeLa cells as described (31).

Transient Expression of Tagged T- and/or L-Plastin in HeLa Cells

The plastin cDNAs and the techniques used for transient expression of the tagged plastin isoforms in HeLa cells were as described elsewhere. Briefly, the plastin cDNAs were obtained by PCR amplification of the DNA generated by reverse transcription of Caco-2 mRNA using isoform-specific oligonucleotides. Epitopes for monoclonal antibodies were added by incorporation of oligonucleotides encoding 11 amino acids of the vesicular stomatitis virus glycoprotein G (T-plastin tag) or 13 amino acids of the sendai virus L protein (L-plastin tag). These tags were specifically recognized by the monoclonal antibodies P5D4 or IV A-2, respectively (14, 41). Standard calcium phosphate techniques were used for transient expression of the cDNAs in HeLa cells.

Infection

Infection of HeLa cells was essentially as described (7). Overnight cultures of *S. flexneri* were diluted into Tryptic soy broth (Diagnostics Pasteur, Marnes la Coquette, France) and grown to mid-exponential phase, centrifuged at 5,000 *g* for 10 min, washed in PBS, and resuspended in MEM to bring the suspension to a concentration of 10^7 cells/ml (M90T, BS176) or 6×10^7 cells/ml (SC300, SC301). HeLa cells grown for 24 h to semi-confluency were washed twice with MEM, and then overlaid with the respective bacterial suspension, followed either by centrifugation for 10 min at 4°C at 780 g (M90T, SC560, BS176), or incubation for 10 min at 4°C (SC300, SC301) to bring bacteria in contact with cells under noninvasive conditions. Unless indicated otherwise, the dishes were then set on top of a 37°C water bath for 30 min (M90T, BS176) or 13 min (SC300, SC301), respectively. Infection was stopped by three washes in PBS at room temperature (rt). For infection of cells previously transfected with the truncated and tagged T-plastin construct (see Fig. 8), bacteria (SC560 or BS176) were used at a concentration of 3×10^6 cells/ml and infection time was 20 min.

Immunofluorescence

For immunofluorescence studies, cells were fixed for 20 min using 3.7% (wt/vol) formaldehyde in PBS. After several washes in PBS, excess aldehyde groups were quenched and cells permeabilized by subsequent incubations at room temperature for 5 min each in PBS/Glycine (0.1 M, pH 7.4), PBS/Triton X-100 (0.1% vol/vol), and PBS. Standard staining procedures for indirect immunofluorescence employed a polyclonal rabbit anti-plastin antibody raised against T-plastin which reacts with both T- and L-plastin (1:400), the anti-tag monoclonal antibodies P5D4 (1:400) and IV A-2 (1:50) as previously described (14, 41), and rhodamine-labeled secondary antibodies (Sigma Chem. Co., St. Louis, MO; 1/80). F-actin was labeled with *N*-(7-nitrobenz-2-oxa-1,3-diazol-4-yl)phallacidin (Molecular Probes, Eugene, OR). The labeled preparations were observed using a conventional fluorescence microscope (BH2-RFCA, Olympus Optical Co., Ltd.) or a confocal laser scanning microscope (Wild Leitz Instruments GmbH, Heidelberg, Germany). Pictures from the latter were recorded on a flat screen monitor with high linearity.

Scanning Electron Microscopy

Cells were fixed for 30 min in 1.6% glutaraldehyde, 1% tannic acid in 0.1 M phosphate buffer (pH 7.4) at rt, rinsed with buffer, and postfixed for 30 min in 1% OsO4 in 0.1 M sodium cacodylate buffer (pH 7.4) at rt. The fixed cells were subsequently dehydrated with ethanol, critical point-dried with carbon dioxide and sputter coated with 3 nm of Pd-Au. Observations were performed using a JEOL 35CF scanning electron microscope operating at 25 kV.

Transmission Electron Microscopy

EM techniques employed to study bacterial entry into HeLa cells were essentially as previously described (68).

Sl-Myosin Decoration of F-Actin

Sl-Myosin prepared as described by Offer et al. (54) was a kind gift of M. F. Carlier (CNRS, Gif, France). Sl-Myosin decoration of filamentous actin was performed as described (68). Briefly, infected cells were exposed to Triton X-100 buffer (1% Triton X-100, 3 mM $MgCl_2$, 30 mM Tris-Cl, pH 8.0) for 10 min at 4°C to remove membranes, incubated for 30 min at 4°C with 8 mg/ml Sl-myosin in 0.1 M phosphate buffer (pH 6.8), washed in 0.1 M phosphate buffer, and fixed in 1% glutaraldehyde, 2% tannic acid, and 50 mM phosphate buffer (pH 6.8). After a wash in 0.1 M phosphate buffer (pH 6.8), the preparation was postfixed in 1% OsO_4 in 0.1 M phosphate buffer (pH 6.3), for 30 min at 4°C, and then rinsed in water, dehydrated, and embedded as described above.

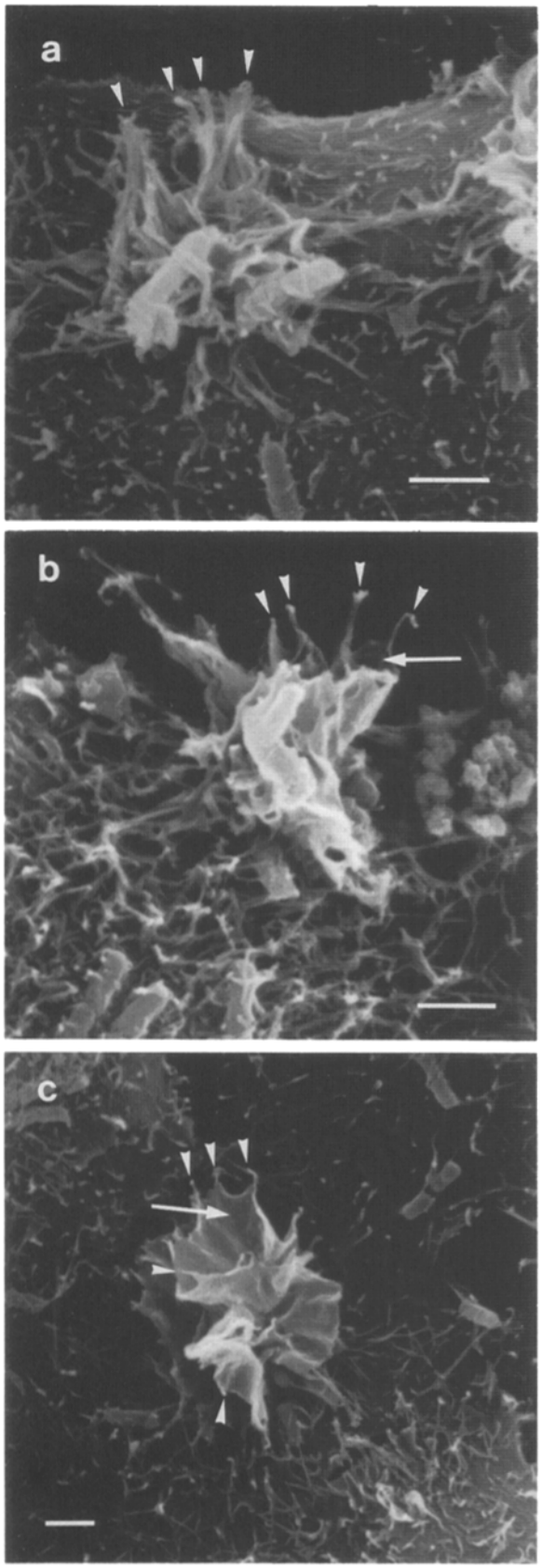

Figure 1. Scanning electron microscopy of *Shigella flexneri*-induced membrane ruffles in HeLa cells (invasive strain SC301): (*a*) accumulation of cellular microspikes that partly stick together to form pillars (*arrowheads*); (*b*) interconnection of the pillars (*arrowheads*) by membrane curtains (*arrow*) that rise between the microspikes; and (*c*) mature, blossom-like structure showing the constitutive elements of ruffle architecture: pillars (*arrowheads*), composed of 2–4 microspikes, and interconnecting membrane sheets (*arrow*). Bars, 2 μm.

Immunogold Labeling

For immunogold labeling of infected HeLa cells, we used a polyclonal antibody raised in rabbit against an NH_2-terminal peptide of α-smooth muscle actin (kind gift of Giulio Gabbiani (University of Geneva, Switzerland); 1:40), or a polyclonal rabbit anti-plastin antibody which was purified against T-plastin but reacts with both T- and L-plastin (1:25), and the technique described by Harding and Geuze (34). In short, the cells were fixed for 2–4 h at 4°C in 1% acrolein and 2% paraformaldehyde in 0.1 M sodium phosphate buffer, pH 7.4, and then immersed overnight in 2.3 M sucrose/PBS. Thin sections were cut at −100°C. The grids were floated on drops of primary antibody diluted in PBS/1% BSA + 1% Tween-20 (pH 7.4). We used a gold-conjugated goat anti-rabbit IgG antibody (EM.GAR 10; British Biocell International, Cardiff, UK), 1:40 diluted in PBS/0.01% gelatin for the labeling step. The preparations were stained for 5 min in 3% uranyl-acetate-oxalate (pH 7.0), rinsed in distilled water, embedded with 1% methyl cellulose (Methocel MC 1.5 mPa.s; Fluka, Switzerland) containing 0.03% uranyl-acetate, air-dried on a loop, and examined in an electron microscope as described above.

HeLa Cell Transfectants Dominant Negative for the T-Plastin Function

Using PCR and conventional cloning techniques, we cloned the 5′-end of a T-plastin cDNA containing only one actin-binding site in frame with the coding sequence for the 11-amino acid peptide tag recognized by the monoclonal antibody P5D4 into the EcoRI and BamHI sites of the eukaryotic expression vector pUHD 15-1 (31) (Fig. 8). We employed standard calcium phosphate precipitation techniques for transient transfection of HeLa cells containing the tetracyclin resistance repressor system (31). No tetracyclin was added to the medium. Therefore, the transfected T-plastin construct was constitutively induced. Thus, we obtained HeLa cells that expressed a functionally inactive, truncated, and tagged T-plastin molecule that competed with the endogenous T-plastin for T-plastin-binding sites on F-actin molecules.

Quantitative Bacterial Entry Assay

To measure bacterial entry into HeLa cells which were or were not transfected with the truncated T-plastin, we infected transiently transfected HeLa cells with the IcsA mutant SC560 in MEM medium for 20 min, and then washed three times with PBS, and incubated the preparation for 2 h in MEM/10% FCS containing Gentamicin (50 μg/ml) to kill extracellular bacteria. The preparation was then fixed and permeabilized as described above. We stained transfected cells with the monoclonal anti-VSV tag antibody, P5D4, and intracellular bacteria with a polyclonal anti-LPS antibody using conventional indirect immunofluorescence techniques. A minimum of a thousand cells was then checked for the expression of the tagged, truncated T-plastin, and for the presence of intracellular bacteria.

Results

During Bacterial Entry, Membrane Ruffles Form Out of Cellular Microspikes, as Seen by Scanning Electron Microscopy

Scanning electron microscopy gave an overall view of the morphological changes on the surface of HeLa cells at *Shigella* entry sites. Fig. 1 *a* shows early formation of cellular microspikes that coalesced to form "pillars." The pillars, generally made of 2–4 microspikes, were interconnected by membrane curtains (Fig. 1 *b*). The mature, blossom-like structure consisted of overlapping membrane sheets that largely surpassed the entering bacterium (Fig. 1 *c*). Interestingly, the skeletal construction could still be recognized at this stage, as the membranous interconnection of the pillars rose from the level of the cytoplasm but did not reach the

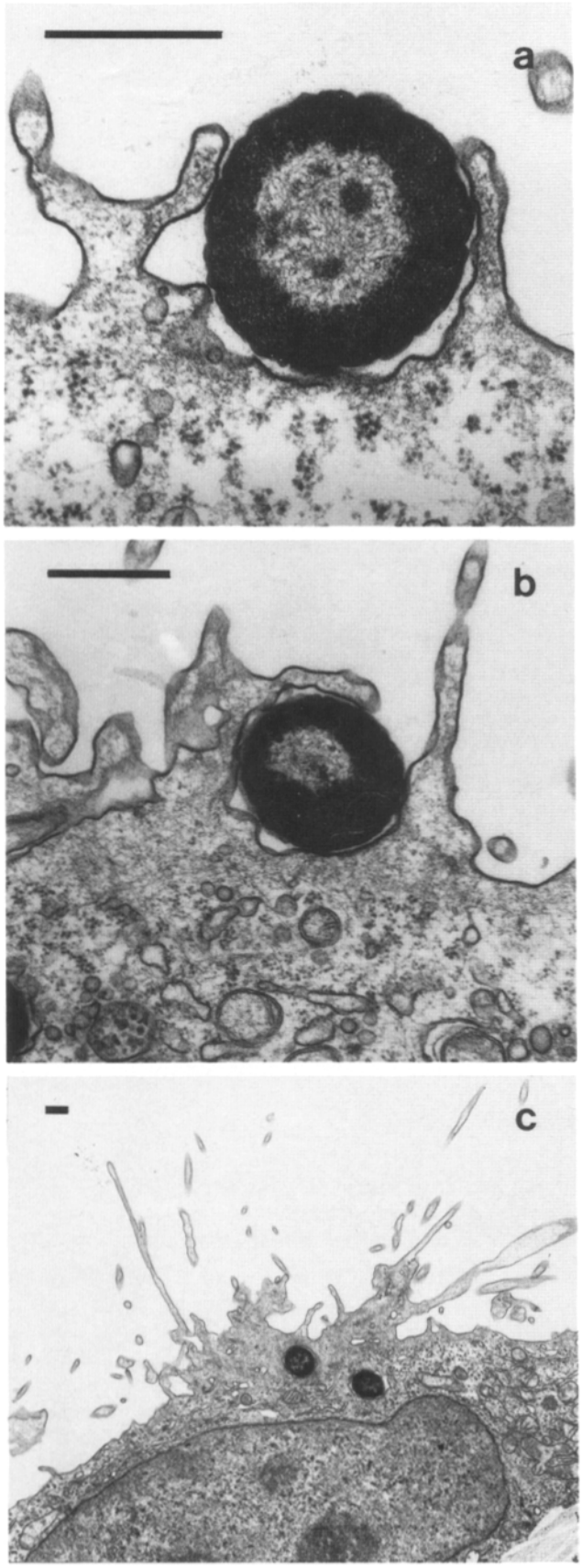

Figure 2. Transmission electron microscopy of *Shigella flexneri* entry into HeLa cells (invasive strain SC301): (*a*) initial pseudopod formation encompassing the bacterium; (*b*) cellular protrusions engulf the bacterium; and (*c*) low magnification view on phagocytized bacteria showing persistence and extension of cellular projections. Bars, 0.5 μm.

very top of the pillars, thus leaving the pillars to overhang. Since the coalescence of 2–4 microspikes to form the pillars also started at the bottom of the cellular projections and was incomplete, even the microspikes that gave rise to the pillars could still be identified (Fig. 1 *c*).

Transmission EM Study of the Entry Process

To study the ultrastructural changes during bacterial entry in more detail, we used conventional transmission electron microscopy to study *Shigella*-infected HeLa cells. Adherence of the pathogenic strain SC301 was followed by the formation of protrusions in the surrounding of the bacterium that extended up to 2 μm along the eukaryotic membrane to each side of the bacterium (Fig. 2, *a* and *b*). The height of the pseudopodia reached 3–5 μm. Thus, the tips of the cellular projections largely exceeded the size of the bacterium (Fig. 2, *b* and *c*). The protrusions next to the bacterium, containing densely packed microfilaments, continued to rise and finally coalesced to engulf the parasite (Fig. 1 *c*). These projections did not always follow the shape of the bacterium but seemed rather to only secondarily get into contact with it (Fig. 2, *a* and *b*). Once the internalization process was completed, the phagocytic vacuole enclosing the parasite remained surrounded by a network of microfilaments (data not shown) while cellular projections at the bacterial entry site persisted (Fig. 2 *c*). The adherent but noninvasive control strain induced only minor membrane projections (Fig. 3 *a*).

Distribution of S1-Myosin-decorated F-Actin during Bacterial Entry

To further characterize the microfilaments involved in cellular uptake of *S. flexneri*, we performed S1-myosin decoration of the filamentous actin of HeLa cells 30 min after bacterial infection. This technique allows one to specifically identify actin filaments, as well as their polarity (68). We were able to observe all stages of bacterial entry in 30 min. Fig. 3 illustrates actin reorganization during these different steps. We observed minor actin accumulation beneath the cell membrane adjacent to the invasive bacterium very early after the infection (Fig. 3 *c*). No actin rearrangement was observed in HeLa cells infected with the noninvasive strain SC300 (Fig. 3 *b*). The next step was characterized by the formation of cellular projections raising beside the bacterium as well as distinct zones of actin nucleation underneath the parasite (Fig. 3, *d* and *e*). The protrusions contained long actin filaments that were all oriented with their barbed ends to the tip of the cellular projection (Fig. 3 *e*). These long filaments sustained the protrusions as they coalesced above the bacterium and maintained these structures even when the phagosome membrane was already destroyed (data not shown). We frequently observed both protrusions beside the bacterium and one or more actin nucleation zones underneath the pathogen (Fig. 3, *d*, *e*, and *f*). Fig. 3 *d* shows two distinct areas packed with electron dense material corresponding to actin-nucleation zones. These zones were scattered along the cytoplasmic membrane in closets with the bacterium. While the structure to the right consists of an ac-

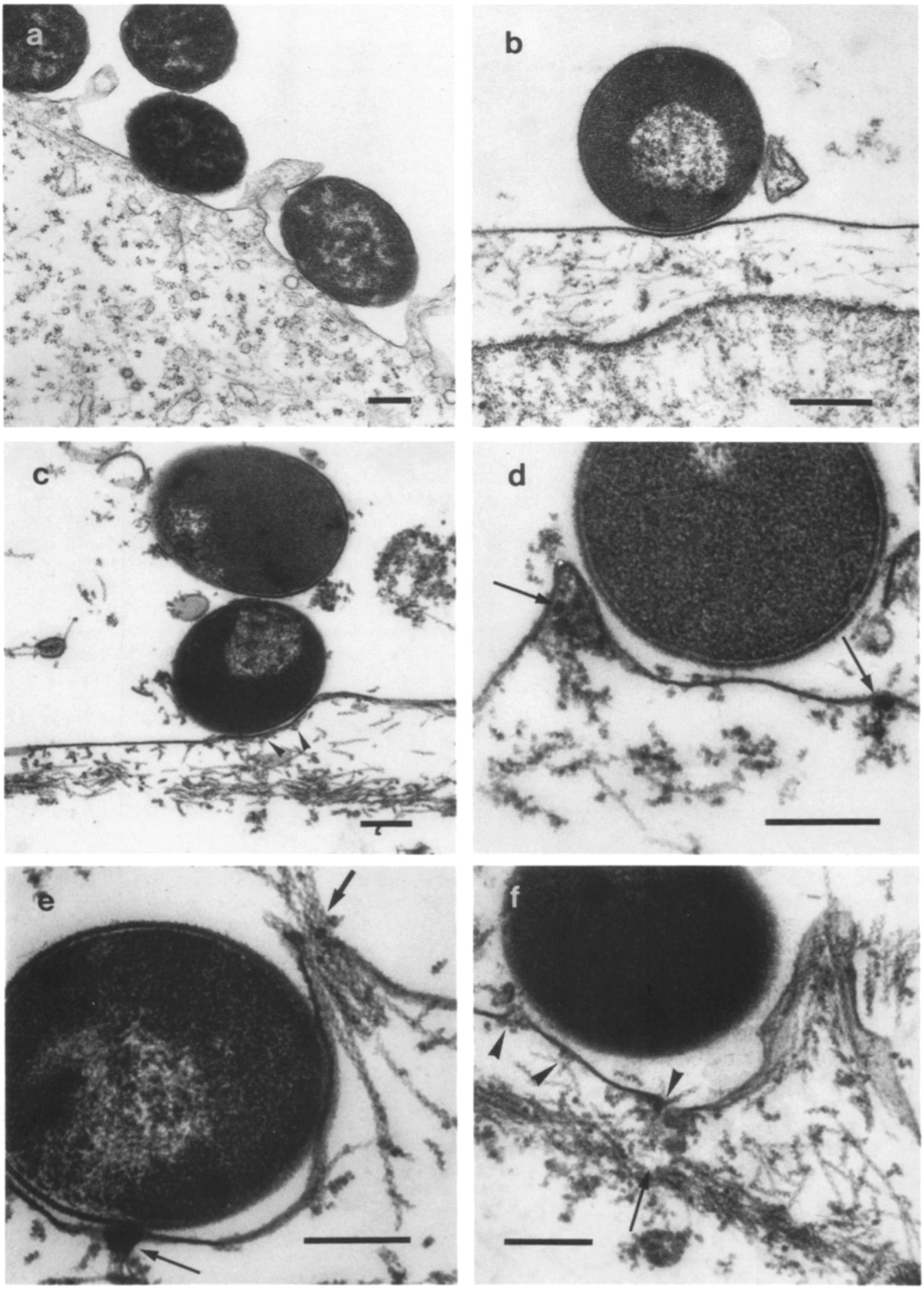

Figure 3. (*a*) Transmission EM-study of noninvasive strain SC300. (*b–f*) EM study of cytoskeletal rearrangements in the host cell during early stages of *Shigella flexneri* invasion into HeLa cells using S1-myosin decoration of F-actin (*b*: noninvasive strain SC300; *c–f*: invasive strain SC301). (*b*) No cytoskeletal rearrangement was seen on physical contact with the cell of noninvasive strain SC300 (control); (*c*) invasive strain SC301 provokes early accumulation of submembranous small actin filaments (*arrowheads*) as the cortical actin layer remains intact; (*d*) discrete actin nucleation foci appear next to the bacterium (*arrows*). Nucleation foci situated beside the bacterium are prone to become cellular protrusions (focus on the left), while nucleation zones under the bacterium evolve into sprinkler-like structures; (*e*) the mature protrusion rising beside the parasite is packed with parallel F-actin filaments whose barbed ends point to the tip of the protrusion (*arrow*). Formation of a sprinkler-like structure below the bacterium (*long arrow*) consisting of actin bundles originating from an actin nucleation zone. Remark membrane fragility at both the tip of the protrusion and the nucleation area below the bacterium; (*f*) alteration of subcortical actin layer (*long arrow*) by one of several actin nucleation zones below the entering bacterium (*arrowheads*). Bars, 0.5 μm.

cumulation of actin nucleation sites with small actin filaments, the zone of heavy actin nucleation to the left is giving rise to a protrusion (*arrows*). If situated under a bacterium, these zones seemed to be at the origin of bundles of actin filaments forming a "sprinkler"-like structure (Fig. 3 *e*, *long arrow*). If situated beside the contact zone of the bacterium and the cell, the presumptive nucleation zone was at the origin of newly formed cellular protrusions containing long actin cables in parallel arrays with barbed ends pointing to the tip of the projections and the densest bundling of actin filaments being observed at the end of the protrusions (Fig. 3, *d*, *e*, and *f*). At this stage, the architecture of the subcortical actin layer may be perturbed (Fig. 3 *f*, *long arrow*).

Plastin Is Recruited into Bacterial Entry Spots

The densely packed F-actin bundles in the cellular protrusions described above suggested the presence of an actin-bundling protein. We used a polyclonal anti-plastin antibody which recognizes both T- and L-plastin, and indirect immunofluorescence labeling of infected HeLa cells, to study the distribution of this protein during infection with *S. flexneri*. After 13 min of infection with the invasive strain SC301, we observed an accumulation of plastin in bacterial entry spots (Fig. 7 *d*). Typically, staining extended far from the center of the invasion zone into pseudopods (see arrows in Fig. 4, *C* and *E*). Even in the occasionally found type of plastin labeling with quite compact staining of the entry spot as represented in Fig. 4 *D*, we regularly saw patterns resembling early stages of pseudopod formation (see arrows in Fig. 4 *D*). Thus, Fig. 4 *D* depicts an early entry event, whereas Fig. 4 *C* represents a more advanced stage in the entry process. Similar results were obtained with the wild-type strain M90T (data not shown). No reorganization of plastin was visible after infection with the avirulent mutants, SC300 (Fig. 4, *A* and *B*) or BS176 (data not shown). The plastin-staining pattern seen in the negative control (Fig. 4 *B*) is not related to bacterial adhesion (Fig. 4 *A*) and reflects normal plastin staining in noninfected cells. In cells, where plastin was rearranged to the entry sites of invasive bacteria, the normal-staining pattern was blurred or invisible (Fig. 4, *C* and *D*). For comparison, we infected HeLa cells with EPEC strain E2348 as described (39), and then fixed and labeled the preparation with the anti-plastin antibody. We used confocal scanning fluorescence microscopy to compare the *Shigella* staining pattern with that of the EPEC strain. Although the EPEC strain also induced an accumulation of plastin at the adherence site, the staining pattern was completely different. In EPEC-infected HeLa cells, the dense staining remained in the very proximity of the bacterial body, after its shape (Fig. 4 *F*, *arrow pointing to one bacterium*), whereas the *Shigella* entry sites clearly reflected plastin labeling of multiple cellular protrusions elicited by a cluster of bacteria interacting with the cell surface (Fig. 4 *E*, *arrows*).

Interestingly, detailed double-labeling studies revealed a slightly differential redistribution of plastin and actin in the bacterial entry spot. As shown in Fig. 7 *g*, plastin concentrates in the tip of the cellular protrusions whereas actin is predominantly found at the base of these bacteria-induced structures (see also Figs. 5 and 6).

Immunogold Labeling Shows Aggregation of Plastin in Cellular Protrusions

To further study the precise localization of plastin in infected HeLa cells, we subjected preparations of infected cells to immunogold labeling with an affinity-purified polyclonal anti-plastin antibody.

At an early entry stage, while cellular protrusions arose next to the bacterium, most of the gold grains were found in the cellular protrusions or in the cytoplasm just underneath (Fig. 5 *a*). The highest concentration of grains seemed to localize in the tip of the projections (Fig. 5 *a*), suggesting an implication of plastin in the formation of tight bundles of actin filaments in cellular projections during the entry process and thus confirming immunofluorescence data shown above (Fig. 7 *g*). At a later stage, after internalization of the parasite, almost all grains were found in cellular protrusions that surrounded the bacterium; only few grains were scattered in the cytoplasm around the phagosome (Fig. 5 *b*). This was in contrast to the labeling pattern seen with an anti-actin antibody which, at an early stage of entry, stained the protrusions as well as the cytoplasm underneath (Fig. 6 *a*). Once the bacterium was in the cell, actin was redistributed into two zones of high actin concentration: (*a*) The protrusions that remained after the internalization of the bacterium, and (*b*) the cellular space in the vicinity of the vacuole containing the parasite (Fig. 6 *b*). These findings indicated differential redistribution of actin and plastin during *Shigella* entry into HeLa cells. While actin and plastin colocalized in the pseudopods, only actin accumulated around the phagosome.

Both Isoforms of Plastin Can Accumulate in Bacterial Entry Sites but Show Different Distribution Patterns

The two isoforms of plastin are differentially expressed in human tissues and cell lines. Leukocytes express L- but not T-plastin; only the T-plastin isoform can be detected in HeLa cells (13). In addition, only L-plastin has hitherto been found to be phosphorylated (13). These findings indicate functional differences of the two plastin isoforms. To see whether both isoforms can similarly be recruited into bacterial entry spots, we transiently transfected HeLa cells with constructs of both T- and L-plastin, each containing an epitope at its COOH-terminal end that is recognized by the monoclonal antibodies (mAb) P5D4 or IV A-2, respectively (14, 41). These mAbs were used to specifically label the respective peptide tags of T- or L-plastin after infection of the transfected cells with SC301 or SC300 (control). As shown in Fig. 7, *a–c* by x-y horizontal sections using confocal fluorescence microscopy, the L-isoform was recruited into the center of the invasion zone whereas the T-isoform was more concentrated in the periphery of the entry zone and reached into the protrusions thus forming a belt around the L-isoform. The differential distribution of the two plastin isoforms was also seen in vertical sections (x-z) where we found that the T-isoform was predominantly recruited to the periphery of the cell while L-plastin was concentrated in greater distance from the cell membrane (Fig. 7 *e*). No differential recruitment of the two plastin isoforms could be seen in double-transfected cells infected with EPEC (Fig. 7), the yellow staining observed, associated to the bacterial body, representing the sum of green and red (i.e., T- and L-plastin).

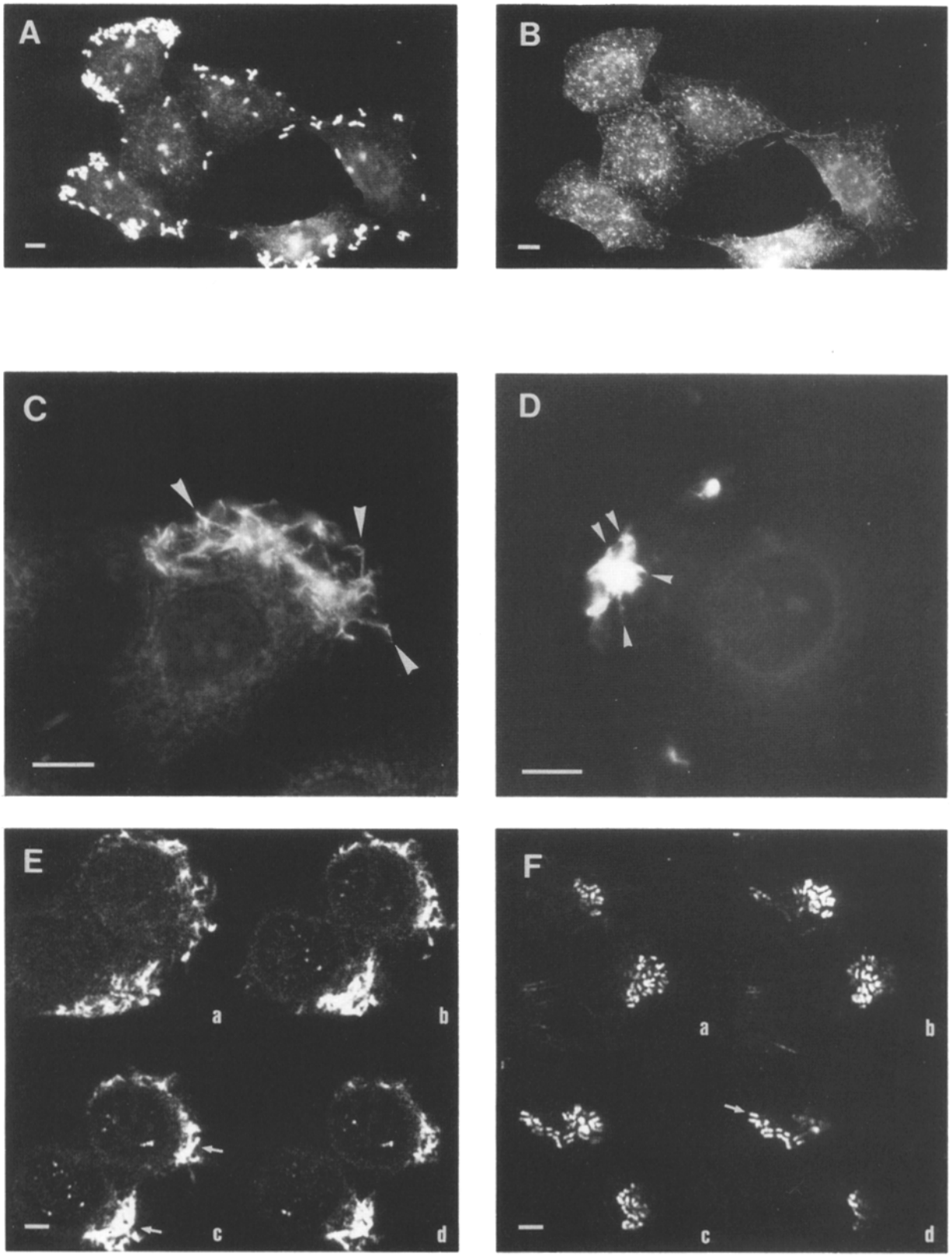

Figure 4. Plastin accumulation in bacterial entry sites of HeLa cells infected with the noninvasive *Shigella* strain SC300 (*A* and *B*), the invasive strain SC301 (*C*, *D*, and *E*), or EPEC (*F*). Conventional (*A–D*) or confocal laser scanning (*E* and *F*) immunofluorescence study using anti-plastin (*B–F*) or anti-LPS (*A*) antibodies. (*A* and *B*) Cells infected with the noninvasive strain SC300 as a negative control show an unaltered plastin-staining pattern (*B*) that is not related to bacterial adherence as shown by parallel labeling of bacteria using an anti-LPS antibody (*A*). (*C*) The invasive strain SC301 induces plastin accumulation in a cell showing several entry spots. The antibody visualizes plastin in a network of cellular protrusions (*arrowheads*) that originate from the bacterial invasion zone. (*D*) Example of plastin aggregation where cellular projections are small (*arrowheads*). This corresponds probably to an earlier entry stage than that shown in *C*. (*E* and *F*) Different staining patterns of plastin in cells infected with invasive *Shigella* (*E*) or EPEC (*F*); confocal laser scan microscopy; width of optical sections, 0.5 μm. In *Shigella* (*E*), plastin localizes preferentially to abundant cellular protrusions elicited by clusters of bacteria interacting with the cell surface (*arrows*), while in EPEC (*F*), only a small zone encompassing each bacterium can be seen (*arrow*). Bars, 4 μm.

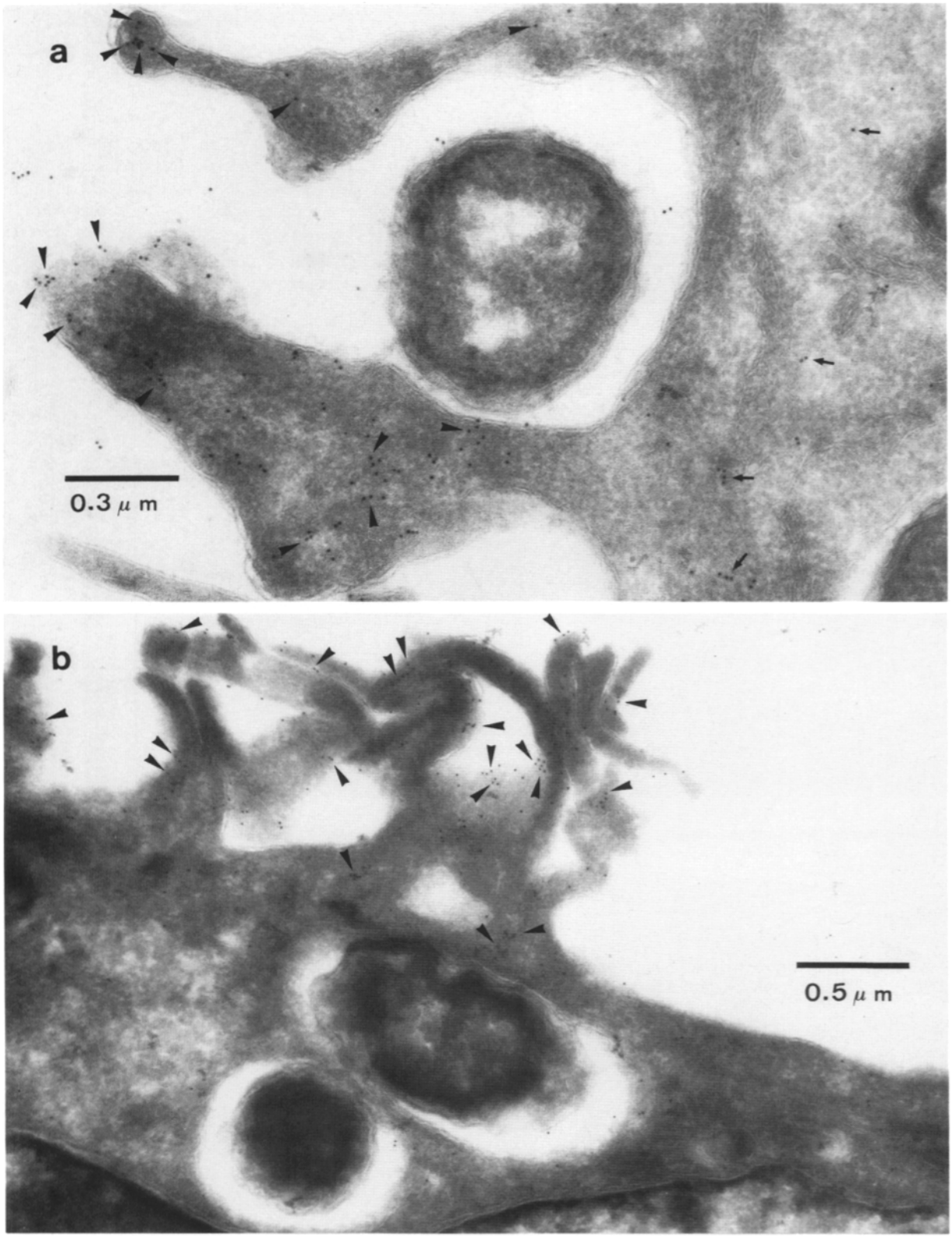

Figure 5. Immunogold labeling of plastin during *Shigella* entry into HeLa cells. (*a*) Early entry stage showing most of the gold grains in cellular protrusions; only a few grains were found in the cytoplasm under the bacterium (*arrowheads*). (*b*) After internalization of the bacterium, almost all gold particles are found in the protrusions (*arrowheads*); note, in contrast to actin, there is an absence of plastin labeling around the parasitic vacuole (Fig. 6 *b*). Bars: (*a*) 0.3 μm; (*b*) 0.5 μm.

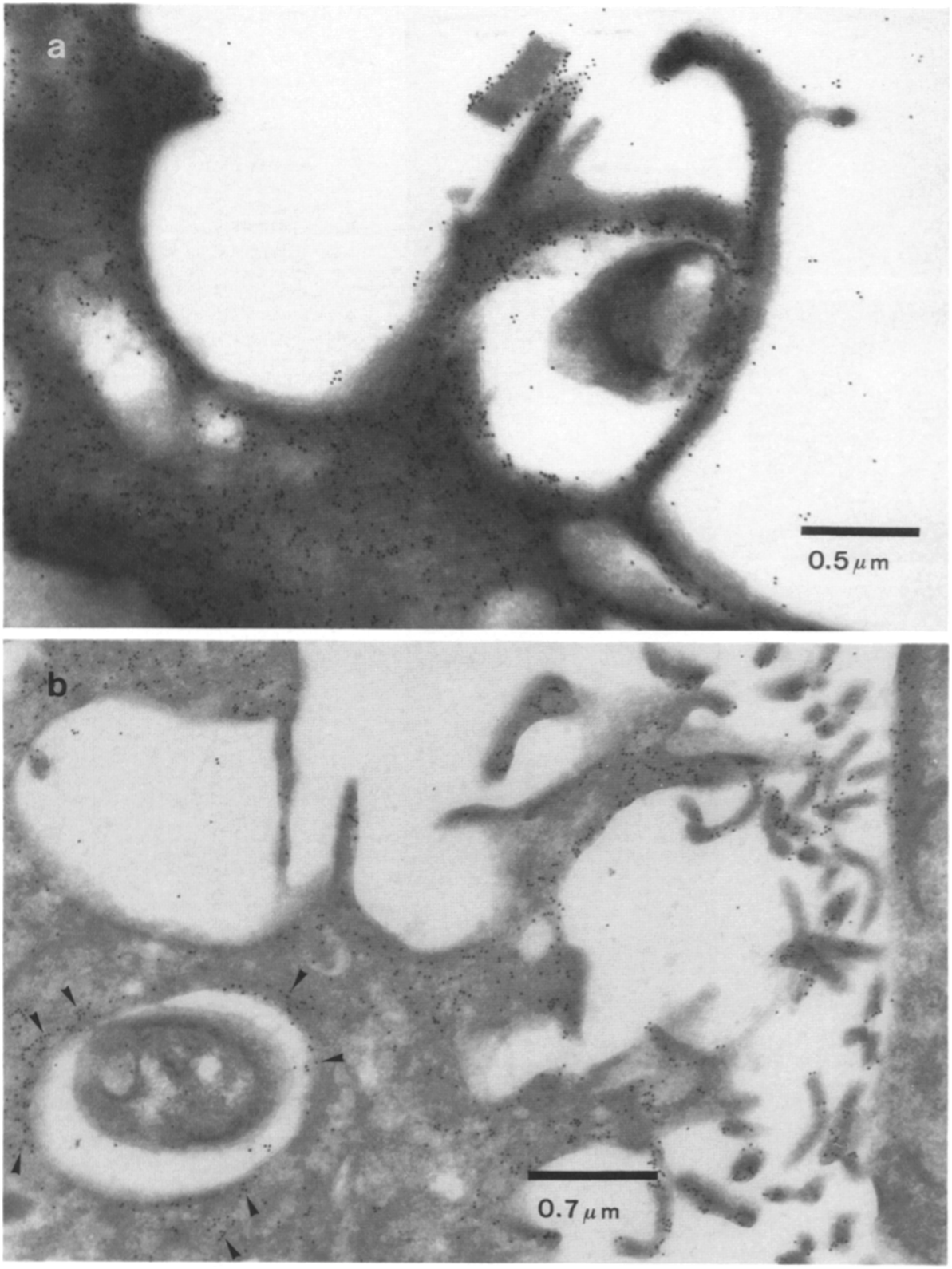

Figure 6. Immunogold labeling of actin during *Shigella* entry into HeLa cells. Entry stages correspond to those shown in Fig. 5. (*a*) Early entry, characterized by actin labeling of cellular protrusions and the cortical cytoplasm underneath. (*b*) Once the bacterium is internalized, actin is not only concentrated in the pseudopods but also around the vacuole containing the bacterium (*arrowheads*) where no plastin accumulation was found (Fig. 5 *b*). Bars: (*a*) 0.5 μm; (*b*) 0.7 μm.

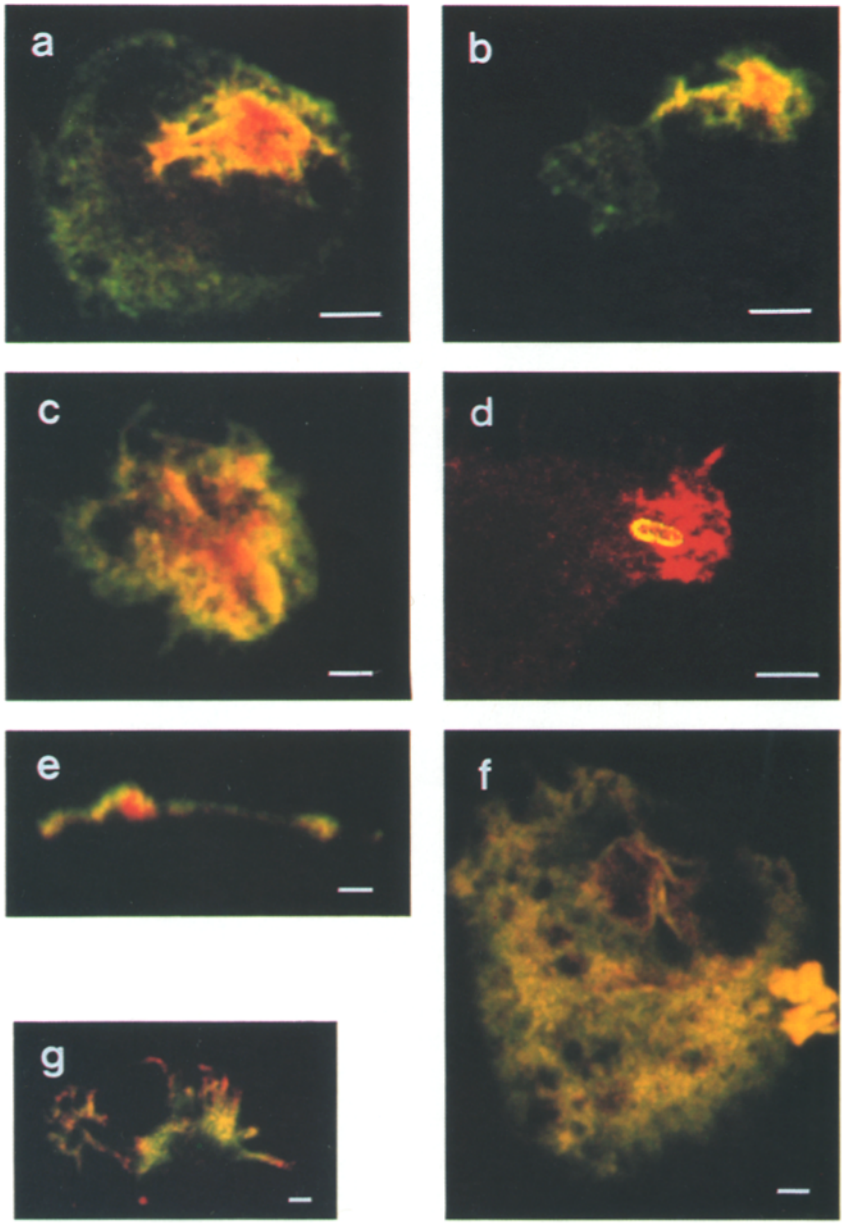

Figure 7. (*a*, *b*, *c*, *e*, and *f*) Double immunofluorescence study showing differential distribution of L- and T-plastin in double-transfected Hela cells during *Shigella* entry by confocal laser scanning microscopy. The cells were transiently double transfected with tag-tailed L- and T-plastin constructions, infected with invasive *Shigella* strain SC301 (*a*, *b*, *c*, and *e*) or EPEC (*f*), fixed, and incubated with the two monoclonal anti-tag antibodies. Secondary antibodies were Texas red for L- and FITC (*green*) for T-plastin; in yellow areas, both plastin isoforms are present. *a* and *b* represent different horizontal (x-y) sections of one *Shigella* entry site, *c* represents an x-y section of a different *Shigella* invasion site; *e* is a vertical (x-z) section of a *Shigella* entry spot, and *f* a horizontal section of an infection site with EPEC. In *Shigella*, the two plastin isoforms are differentially recruited into the entry site: L-plastin (*red*) stains predominantly the center of the invasion site as well as the base and core of the protrusions while T-plastin (*green*) is found in the periphery, especially in the tips of cellular protrusions (*a*, *b*, and *c*). (*e*) The vertical section of a *Shigella* invasion site shows compact L-plastin in the center while T-plastin is situated more in the periphery of the site. (*f*) EPEC, in contrast to *Shigella*, recruits both T- and L-plastin isoforms similarly, as indicated by the yellow area encompassing the bacteria. (*d*) *Shigella flexneri* (anti-LPS/FITC) and plastin (polyclonal anti-plastin/Texas red) colocalize in a bacterial entry spot as seen in a horizontal section using confocal laser scan microscopy. (*g*) Double immunofluorescence study of plastin (polyclonal anti-plastin/Texas red) and actin (NBD-phallacidine) in *Shigella* entry spots. Confocal laser scan microscopy shows differential recruitment of plastin and actin into bacterial entry spots with plastin staining preferentially the tips of the protrusions while actin is concentrated at the base of cellular projections. Bars, 2 μm. Width of optical sections: 0.3 μm.

T-Plastin Is Essential for Shigella Entry into HeLa Cells

The differential recruitment of T- and L-plastin into bacterial entry spots, the T-isoform concentrated in the tips of the cellular protrusions and L-plastin more at the base of these structures (Fig. 7, *a–c*, and *e*), and published data suggesting the presence of T- but not of L-plastin in HeLa cells (13) prompted us to hypothesize that T-plastin is important for bacterial entry into HeLa cells. To obtain HeLa cells dominant negative for the T-plastin function, we expressed a truncated and tagged T-plastin construct that was designed to compete with the endogenous protein for actin binding (Fig. 8). After tranfection of HeLa cells with the T-plastin truncate, we infected the cells with the invasive but nonmotile mutant SC560 (IcsA$^-$). This strain was used in order to prevent cell–cell spread of the bacteria (2, 30, 57). We also infected with BS176, a noninvasive, virulence-plasmid cured mutant, as a negative control. We identified transfected cells using the anti-tag mAB P5D4 (41), nontransfected cells by negative P5D4 labeling and phase contrast microscopy, and infected cells by a bacterial stain using an anti-LPS antibody. We observed a significant inhibition by 64% of entry into transfected cells of the invasive strain SC560 as compared to nontransfected cells (Fig. 9, $p < 0.05$). The noninvasive strain BS176 was negative for invasion of transfected or nontransfected cells. No morphological alterations were observed in transfected vs nontransfected HeLa cells.

Discussion

Entry processes into eukaryotic cells of facultatively intracellular bacteria as different as *Shigella*, *Yersinia*, *Salmonella*, and enteroinvasive *E. coli*, require actin polymerization (7, 8, 18, 21, 24, 40, 68, 71). The goal of this work was

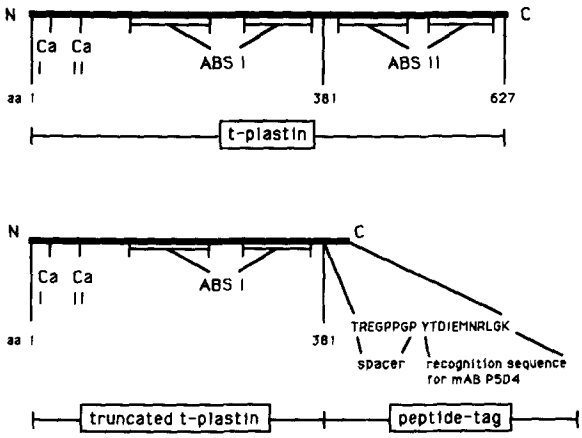

Figure 8. Schematic representation of the truncated T-plastin construct used for transfections. Plastin contains two tandem putative actin-binding sites (*ABS I* and *ABS II*) as well as consensus sequences for calmodulin-like calcium-binding sites (*Ca I* and *Ca II*). We replaced the second actin-binding site (*ABS II*) by a peptide tag consisting of an 8-amino acid long spacer and the recognition sequence of the monoclonal antibody P5D4 (11 aa.) at the COOH terminus.

Inhibition of Shigella entry into HeLa cells dominant negative for T-plastin function

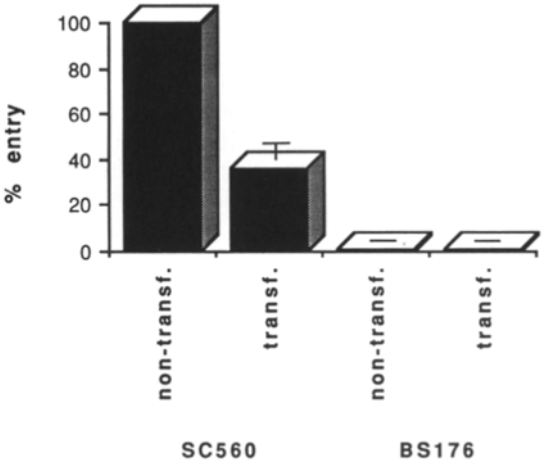

Figure 9. Inhibition of *Shigella* entry by expression of a nonfunctional T-plastin truncate in HeLa cells. HeLa cells dominant negative for the T-plastin function by transfection with the truncated and tagged T-plastin construct (see Fig. 8) are less susceptible to infection with the invasive strain SC560 in comparison to nontransfected cells. Represented are the arithmetic means of four experiments. Error bars indicate +SD. Entry values for nontransfected cells infected with the invasive strain C560 (positive control) were normalized to 100%. The noninvasive control strain BS176 was negative for infection of both transfected and nontransfected cells.

to better understand *Shigella*-induced cytoskeletal rearrangements and their similarity to physiological patterns of cell behavior like phagocytosis or formation of brush border microvilli.

After initial contact of *S. flexneri* with the HeLa cell membrane, several distinct nucleation zones of actin polymerization were seen within or adjacent to the plasma membrane. Surprisingly, the cellular protrusions were not formed as a continuous wave-like structure encompassing the parasite but rather resulted from a discontinuous process of scattered actin nucleation in or underneath the cytoplasmic membrane next to the entering bacterium (Fig. 3, *d*, *e*, and *f*). The outcome of the initial nucleation event seemed to depend on the location of the nucleation site with regard to the bacterium: nucleation foci arising beside the bacterium resulted in a cellular protrusion, whereas nucleation zones immediately under the bacterium ended up in a sprinkler-like structure characterized by a bouquet of actin filaments originating in a nucleation zone at the membrane (Fig. 3, *d*, *e*, and *f*). The nucleation zone of developing protrusions vanished as long actin filaments erected the cellular protrusions. In contrast, nucleation zones under the bacterium that gave rise to the sprinkler-like structures remained for a certain period of time (Fig. 3 *e*).

On a larger scale, the scattered actin nucleation and formation of protrusions corresponded to the high density of cellular microvilli around the entering bacterium (Fig. 1 *a*). Microvilli are the morphological basis of the *Shigella*-induced entry structure since they were seen to coalesce and form pillars bearing the overlapping membrane leafs that are characteristic for the mature, blossom-like entry complex (Fig. 1, *a–c*). The overall morphology of the mature structure resembled HEp-2 cell membrane ruffles during *Salmonella* invasion (20, 21). However, it is not known if *Salmonella*-induced ruffles are the result of pillar formation with subsequent membranous interconnection as described here, or are due to homogenous wave-like membranous extensions of the cell. Given the different features observed during entry of the two enteroinvasive bacteria: *Salmonella* elicits a cellular calcium flux–*Shigella* does not (4, 56); *Salmonella* penetrates polarized epithelial cells by the apical pole–*Shigella* by the basolateral pole (17, 53, 66), it would not be surprising to find somewhat distinct entry mechanisms of the two pathogens.

It is not yet clear whether the discontinuous actin nucleation foci around the entering bacterium are due to a cellular nucleator activated by a *Shigella*-triggered transmembrane signal, or due directly to a bacterial nucleator able to cross the cytoplasmic membrane. An argument for the latter mechanism is the finding that one of the bacterial pathogenicity determinants, IpaB, is associated with both contact hemolysis and entry into epithelial cells (10, 36). Thus, it is possible that IpaB provides access to the cytoplasm for a bacterial nucleator, or is the bacterial nucleator itself. As to the discontinuity of the process, one might speculate that the concentration of one of the components of the signaling system becomes critical for signal transduction; be it a bacterial effector, an element of a cellular transmembrane signaling system, an actin-binding protein, G-actin, or any regulator involved in the system.

Initially, the discontinuous process of actin nucleation did not affect the integrity of the network of subcortical F-actin. As entry proceeded, long actin cables were formed out of nucleation foci, giving rise to either a cellular protrusion or a sprinkler-like structure according to the situation of the

nucleation focus. At this stage, the integrity of subcortical actin was disturbed. *Shigella*-induced cellular protrusions were characterized by long densely bundled actin filaments organized in parallel orientation with their barbed ends pointing to the tip of the protrusions (Fig. 3, *e* and *f*). At this step, the initial nucleation zone that gave rise to the protrusion had already vanished. We speculate that initial parasite-induced actin nucleation results in small actin filaments that are neither spatially oriented nor bound to the membrane. Some of them may gain access to an actin-binding site of the membrane. These filaments would continue to polymerize actin predominantly at the barbed end and thus help erect the protrusion while free filaments are depolymerized, providing a G-actin pool for the formation of the protrusion.

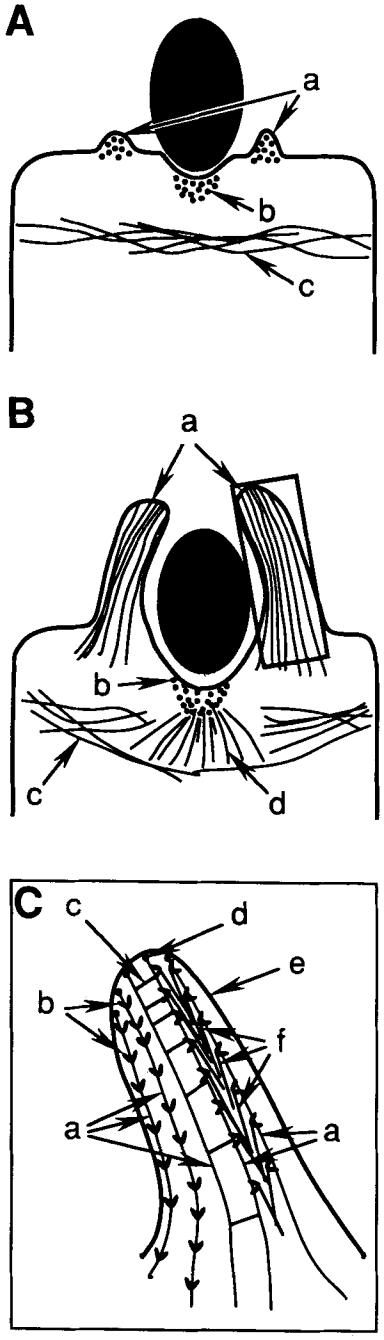

The striking feature of tightly bundled actin filaments in parallel orientation with their barbed ends pointing to the tip of the protrusions as the major morphological constituent of the bacteria-induced pseudopodia resembled the microarchitecture of microvilli of the intestinal brush border (52). In chicken brush border, F-actin bundling is mediated by villin and fimbrin (52). Villin plays a key role in the morphology of intestinal microvilli, but is not expressed in HeLa cells (22, 23). Fimbrin tightly bundles actin filaments in arrays of parallel orientation (28, 49) and is necessary for in vitro reassociation of microvillar core proteins (12). The observation that the F-actin in the cellular protrusions was tightly bundled in parallel arrays suggested a possible involvement in the architecture of the bacteria-induced cellular protrusions of an actin-bundling protein of the fimbrin family. Plastin belongs to this family of actin-bundling proteins, including T- and L-plastin and fimbrin (5, 6, 13, 45, 46). Amino acid sequence analysis of plastin reveals two closely associated presumptive actin-binding sites as well as two hypothetical calcium-binding sites (13, 45), which makes this protein the best candidate for very tight packing of actin filaments. Thus, we studied the role of plastin for *Shigella* entry into epithelial cells. Immunofluorescence labeling showed accumulation of plastin in *Shigella* entry spots (Fig. 4, *C*, *D*, and *E*). Using immunogold labeling of cryosections

Figure 10. Hypothetical model of cytoskeletal rearrangements during entry of *Shigella flexneri* into HeLa cells. (*A*) Early entry stage. (*a*) Lateral zone of actin nucleation; (*b*) actin nucleation site under the bacterium; (*c*) subcortical actin filaments. The bacterium induces the formation of actin nucleation zones that are disseminated beside (*a*) or under (*b*) the parasite. Subcortical actin filaments (*c*) remain intact. (*B*) Later entry stage. (*a*) Bacteria-induced cellular protrusions; (*b*) actin nucleation zone; (*c*) subcortical actin filaments; (*d*) actin filaments nucleated by *b*. Some of the short actin filaments formed in nucleation sites beside the bacterium gain access and are fixed to the membrane by their barbed ends. These filaments continue to polymerize thus forming cellular protrusions that encompass the bacterium (*a*). The nucleated actin filaments of lateral nucleation zones that remain in the cytoplasm are depolymerized to add to the G-actin pool used for the construction of the protrusions (not shown). The actin nucleation zone under the bacterium, however, remains intact (*b*). It gives rise to a bunch of actin filaments (*d*) thus showing the aspect of a sprinkler-like structure (*b*+*d*). We hypothesize that nucleation foci situated directly under the membrane (e.g., that at the tip of arrow *b*) remain "sterile" in lack of cortical G-actin which is completely incorporated into the long actin filaments forming the protrusions whereas the formation of the bunch of actin cables from the bottom of the nucleation zone is fueled by G-actin that comes from depolymerized subcortical actin filaments (*c*). (*C*) Microarchitecture of a cellular protrusion (see *B*, *a*). (*a*) Actin filaments; (*b*) S1-myosin (to show the orientation of actin filaments); (*c*) plastin; (*d*) unknown molecule that binds actin filaments to the cell membrane; (*e*) cell membrane; (*f*) myosin. Bacteria-induced pseudopods are formed by long, parallel actin filaments (*a*) that point with their barbed ends to the tip of the protrusion as determined by S1-myosin decoration (*b*). Parallel actin filaments are tightly bundled by plastin (*c*) and their barbed ends bound to the cell membrane (*e*) by an unknown molecule (*d*). Once the protrusions fuse above the bacterium, actin filaments span from the bottom of the former protrusions to the top of the newly formed vacuole (see *B*). An actin/myosin (*f*)-based filament movement then draws the parasitic vacuole into the cell.

and electron microscopy, we found actin in both cellular protrusions and all around the invaginating vacuole whereas plastin was spotted only in the protrusions where it serves bundling the actin filaments (Figs. 5 and 6). For now, we do not know if this is due to distinct signaling pathways or to differential distribution patterns of these proteins in the cell. We also do not know if plastin has the morphogenic potential to generate the formation of the protrusions. In yeast, the morphogenic potential of the plastin homologue Sac6p has been shown (1).

Both T- and L-plastin can be recruited into the bacterial entry site when HeLa cells are transfected with either of the isoforms. Since the mRNA of L-plastin has not been found in HeLa cells (13), it is probably the T-isoform that accumulates in the cellular protrusions formed during HeLa cell infection with *S. flexneri*. This goes well with the analysis in the confocal microscope of HeLa cells double transfected with both plastin isoforms showing a different pattern of recruitment into the bacterial entry site for L- or T-plastin: while the L-isoform was recruited into the center of the bacterial invasion zone, the T-isoform was located in the periphery of the entry zone. Furthermore, in vertical sections, L-plastin was found more towards the center of the cell. In contrast, the T-isoform accumulated at the cell border. Thus, the T-isoform seems to be recruited into the protrusions where it serves bundling long actin filaments in parallel arrays while the L-isoform remains in the body of the infected cell. The differential intracellular distribution of the two plastin isoforms might reflect distinct binding specificities of the two proteins. The T-isoform would organize parallel actin filaments into bundles as found in the protrusions, whereas the L-isoform would be implicated in the formation of complex structures like subcortical actin. Further studies are necessary to elucidate the regulation of the plastin accumulation described here.

While the functional role for the bacterial entry process of cellular protrusions seems obvious, the precise function of the sprinkler-like structure below the bacterium remains elusive. It might reflect an abortive protrusion. However, the occasional observation that the subcortical actin below a sprinkler-like structure remained intact forming a network with the sprinkler filaments (data not shown) may indicate a more active role in the bacterial entry process of this structure. Thus, this network could be part of substantial remodeling of subcortical actin being necessary to attract the macropinocytotic vacuole into the cell.

Using dominant negative transient transfectants and a quantitative entry assay, we have provided evidence for the functional role of T-plastin for the cytoskeletal rearrangements during bacterial entry. HeLa cells, transfected with a truncated T-plastin which was devoid of one of its two actin-binding sites and thus unable to bundle actin filaments, were significantly less susceptible to infection with *S. flexneri*, thus proving the functional role of this plastin-isoform for bacterial entry. Since the T-isoform is concentrated in the cellular projections surrounding the entering bacterium, the experiments demonstrate that it is the T-isoform that bundles actin filaments in these parasite-induced microvilli and that actin bundling in the bacteria-induced protrusions is essential for efficient *Shigella* entry into HeLa cells. In the course of this study, the EPEC strain was used only as a control, demonstrating that foci of bacteria-cell interaction were not all similar. Significance of the strict colocalization of the two plastin isoforms in the case of EPEC is not understood, although it certainly reflects a significant difference in reorganization of the cytoskeleton. Within the limits of this study, the weak efficiency of EPEC invasion, as compared to *Shigella*, precluded the use of truncated plastin expression for *trans*-dominant negative effect.

Based on some of the above presented morphological and functional data and the published observation that myosin can be found in *Shigella* entry spots (7), we propose a model for the cytoskeletal rearrangements during *Shigella flexneri* invasion of HeLa cells (Fig. 10). Since a number of bacterial determinants conferring the invasive phenotype is known, we believe that the *Shigella* entry system provides a valid tool to study further cytoskeletal functions of eukaryotic cells.

We thank M.-F. Carlier (Centre National de la Recherche Scientifique, Gif-sur-Yvette, France) for the preparation of S1-myosin. We are indebted to R. Hellio (Unité de Biologie des Membranes, Institut Pasteur, Paris) who performed laser scanning microscopy, to J. Mounier (Unité de Pathogénie Microbienne Moléculaire, Institut Pasteur, Paris) for excellent technical help, and to C. Rolin (Station Centrale de Microscopie Electronique, Institut Pasteur, Paris) for expert photographic work. W. Neubert (Max Planck Institut für Biochemie, Martinsried, Germany), T. Kreis (Département de Biologie Cellulaire, Université de Genève, Switzerland), and G. Gabbiani (Département de Pathologie, Université de Genève, Switzerland) kindly provided us with antibodies. We are indebted to H. Bujard (Zentrum für Molekulare Biologie, Universität Heidelberg, Germany) for the plasmid pUHD15-1 and tTA-transfected HeLa cells. We thank T. Vasselon and N. Mantis for critical reading of the manuscript.

T. A. has been a recipient of post-doctoral fellowships from the Deutsche Forschungsgemeinschaft (DFG: Ad 95, 1-1) and the European Community (EC: ERBCHRXCT 930255).

Received for publication 20 July 1994 and in revised form 13 January 1995.

References

1. Adams, A. E. M., D. Botstein, and D. G. Drublin. 1991. Requirement of yeast fimbrin for actin organization and morphogenesis in vivo. *Nature (Lond.).* 354:404–408.
2. Bernardini, M. L., J. Mounier, H. d'Hauteville, M. Coquis-Rondon, and P. J. Sansonetti. 1989. Identification of *icsA*, a plasmid locus of *Shigella flexneri* that governs bacterial intra- and intercellular spread through interaction with F-actin. *Proc. Natl. Acad. Sci. USA.* 86:3867–3871.
3. Bernardini, M. L., M. G. Sanna, A. Fontaine, and P. J. Sansonetti. 1993. OmpC is involved in invasion of epithelial cells by *Shigella flexneri*. *Infect. Immun.* 61:3625–3635.
4. Boyles, J., and D. F. Bainton. 1981. Changes in plasma membrane-associated filaments during endocytosis and exocytosis in polymorphonuclear leukocytes. *Cell.* 24:905–914.
5. Bretscher, A. 1981. Fimbrin is a cytoskeletal protein that crosslinks F-actin in vitro. *Proc. Natl. Acad. Sci. USA.* 78:6849–6853.
6. Bretscher, A., and K. Weber. 1980. Fimbrin, a new microfilament-associated protein present in microvilli and other surface structures. *J. Cell Biol.* 86:335–340.
7. Clerc, P., and P. J. Sansonetti. 1987. Entry of *Shigalla flexneri* into HeLa cells: evidence for directed phagocytosis involving actin polymerization and myosin accumulation. *Infect. Immun.* 55:2681–2688.
8. Clerc, P., and P. J. Sansonetti. 1988. Entry of *Shigella flexneri* into epithelial cells: evidence for induced phagocytosis involving actin and myosin. Colloque INSERM, Vol. 171. Structure and Functions of the Cytoskeleton. Bernard A. F. Rousset, editor. John Libbey Eurotext.
9. Clerc, P., and P. J. Sansonetti. 1989. Evidence for clathrin mobilization during directed phagocytosis of *Shigella flexneri* by HEp2 cells. *Microb. Pathog.* 7:329–336.
10. Clerc, P., B. Baudry, and P. J. Sansonetti. 1986. Plasmid-mediated contact haemolytic activity in *Shigella* species: correlation with penetration into HeLa cells. *Ann. Inst. Pasteur Microbiol.* 137 A:267–278.
11. Clerc, P., B. Berthon, M. Claret, and P. J. Sansonetti. 1989. Internalization of *Shigella flexneri* into HeLa cells occurs without an increase in cytosolic Ca^{2+} concentration. *Infect. Immun.* 57:2919–2922.
12. Coluccio, L. M., and A. Bretscher. 1989. Reassociation of microvillar core proteins: making a microvillar core in vitro. *J. Cell Biol.* 108:495–502.

13. De Arruda, M. V., S. Watson, C. S. Lin, J. Leavitt, and P. Matsudaira. 1990. Fimbrin is a homologue of the cytoplasmic phosphoprotein plastin and has domains homologous with calmodulin and actin gelation proteins. *J. Cell Biol.* 111:1069–1079.
14. Einberger, H., R. Mertz, P. H. Hofschneider, and W. J. Neubert. 1990. Purification renaturation, and reconstituted protein kinase activity of the Sendai virus large (L) protein: L protein phosphorylates the NP and P proteins in vitro. *J. Virol.* 64:4274–4280.
15. Finlay, B. B., and S. Falkow. 1988. A comparison of microbial invasion strategies of *Salmonella, Shigella* and *Yersinia* species. *Mol. Cell. Biol.* 64:227–243.
16. Finley, B. B., and S. Falkow. 1988. Comparison of the invasion strategies used by *Salmonella cholerae-suis, Shigella flexneri* and *Yersinia enterocolitica* to enter cultured animal cells: endosome acidification is not required for bacterial invasion or intracellular replication. *Biochimie.* 70:1089–1099.
17. Finlay, B. B., J. Fry, E. P. Rock, and S. Falkow. 1989. Passage of *Salmonella* through polarized epithelial cells: role of the host and bacterium. *J. Cell Sci. Suppl.* 11:99–107.
18. Finlay, B. B., K. Y. Leung, I. Rosenshine, and F. Garcia-del Portillo. 1992. *Salmonella* interactions with the epithelial cell. *ASM News.* 58:486–489.
19. Francis, C. L., A. E. Jerse, J. B. Kaper, and F. Stanley. 1991. Characterization of interactions of enteropathogenic *Escherichia coli* O127:H6 with mammalian cells in vitro. *J. Inf. Dis.* 164:693–703.
20. Francis, C. L., T. A. Ryan, B. D. Jones, S. J. Smith, and S. Falkow. 1993. Ruffles induced by *Salmonella* and other stimuli direct macropinocytosis of bacteria. *Nature (Lond.).* 364:639–642.
21. Francis, C. L., M. N. Starnbach, and S. Falkow. 1992. Morphological and cytoskeletal changes in epithelial cells occur immediately upon interaction with *Salmonella typhimurium* grown under low-oxygen conditions. *Mol. Microbiol.* 6:3077–3087.
22. Franck, Z., M. Footer, and A. Bretscher. 1990. Microinjection of villin into cultured cells induces rapid and long-lasting changes in cell morphology but does not inhibit cytokinesis, cell motility, or membrane ruffling. *J. Cell Biol.* 111:2475–2485.
23. Friedrich, E., C. Huet, M. Arpin, and D. Louvard. 1989. Villin induces microvilli growth and actin redistribution in transfected fibroblasts. *Cell.* 59:461–475.
24. Gaillard, J. L., P. Berche, C. Fréhel, E. Gouin, and P. Cossart. 1991. Entry of *Listeria monocytogenes* into cells is mediated by internalin, a repeat protein reminiscent of surface antigens from Gram-positive cocci. *Cell.* 65:1127–1141.
25. Gaillard, J. L., P. Berche, J. Mounier, S. Richard, and P. J. Sansonetti. 1987. In vitro model of penetration and intracellular growth of *Listeria monocytogenes* in the human enterocyte-like cell line Caco2. *Infect. Immun.* 55:2822–2829.
26. Galan, J. E., J. Pace, and M. J. Hayman. 1992. Involvement of the epidermal growth factor receptor in the invasion of cultured mammalian cells by *Salmonella typhimurium. Nature (Lond.).* 357:588–589.
27. Gemski, P. J., A. Takeuchi, O. Washington, and S. B. Formal. 1972. Shigellosis due to *Shigella dysenteriae* 1: relative importance of the mucosal invasion versus toxin production in pathogenesis. *Infect. Dis.* 126:523–530.
28. Glenney, J. R., P. Kaulfus, P. Matsudaira, and K. Weber. 1981. F-actin binding and bundling properties of fimbrin, a major cytoskeletal protein of microvillus core filaments. *J. Biol. Chem.* 256:9283–9288.
29. Goldberg, M., and P. J. Sansonetti. 1993. Shigella subversion of the cellular cytoskeleton: a strategy for epithelial colonization. *Infect. Immun.* 61:4941–4946.
30. Goldberg, M. B., O. Bârzu, C. Parsot, and P. J. Sansonetti. 1993. Unipolar localization and ATPase activity of IcsA, a *Shigella flexneri* protein involved in intracellular movement. *J. Bacteriol.* 175:2189–2196.
31. Gossen, M., and H. Bujard. 1992. Tight control of gene expression in mammalian cells by tetracycline-responsive promoters. *Proc. Natl. Acad. Sci. USA.* 89:5547–5551.
32. Hale, T. L., R. E. Morris, and P. F. Bonventre. 1979. *Shigella* infection of Henle intestinal epithelial cells: role of the host cell. *Infect. Immun.* 24:887–894.
33. Hansen, S. H., K. Sandvig, and B. van Deurs. 1993. Clathrin and HA2 adaptors: effects of potassium depletion, hypertonic medium, and cytosol acidification. *J. Cell Biol.* 121:61–72.
34. Harding, C. V., and H. J. Geuze. 1992. Class II MHC molecules are present in macrophage lysosomes and phagolysosomes that function in the phagocytic processing of *Listeria monocytogenes* for presentation to T cells. *J. Cell Biol.* 119:531–542.
35. Heesemann, J., and R. Laufs. 1985. Double immunofluorescence microscopic technique for accurate differentiation of extracellularly and intracellularly located bacteria in cell cultures. *J. Clin. Microbiol.* 22:168–175.
36. High, N., J. Mounier, M. C. Prévost, and P. J. Sansonetti. 1992. IpaB of *Shigella flexneri* causes entry into epithelial cells and escape from the phagocytic vacuole. *EMBO (Eur. Mol. Biol. Organ.) J.* 11:1991–1999.
37. Isberg, R. R., and J. M. Leong. 1990. Multiple β_1 chain integrins are receptors for invasin, a protein that promotes bacterial penetration into mammalian cells. *Cell.* 60:861–871.
38. Kadurugamuwa, J. L., M. Rohde, J. Wehland, and K. Timmis. 1991. Intercellular spread of *Shigella flexneri* through a monolayer mediated by membranous protrusions and associated with reorganization of the cytoskeletal protein vinculin. *Infect. Immun.* 59:3663–3671.
39. Knutton, S., T. Baldwin, P. H. Williams, and A. S. McNeish. 1989. Actin accumulation at sites of bacterial adhesion to tissue culture cells: basis of a new test for enteropathogenic and enterohemorrhagic *Escherichia coli. Infect. Immun.* 57:1290–1298.
40. Knutton, S., P. H. Williams, D. R. Lloyd, D. C. A. Candy, and A. S. McNeish. 1984. Ultrastructural study of adherence to and penetration of cultured cells by two invasive *Escherichia coli* strains isolated from infants with enteritis. *Infect. Immun.* 44:559–608.
41. Kreis, T. E. 1986. Microinjected antibodies against the cytoplasmic domain of vesicular stomatitis virus glycoprotein block its transport to the cell surface. *EMBO (Eur. Mol. Biol. Organ.) J.* 5:931–941.
42. Kübler, E., and H. Riezman. 1993. Actin and fimbrin are required for the internalization step of endocytosis in yeast. *EMBO (Eur. Mol. Biol. Organ.) J.* 12:2855–2862.
43. Labigne-Roussel, A. F., L. Lark, G. Schoolnik, and S. Falkow. 1984. Cloning and expression of an afimbrial adhesin (AFA) responsible for P blood group-independent mannose-resistant hemagglutination from a pyelone-phritic *E. coli* strain. *Infect. Immun.* 46:251–259.
44. LaBrec, E. H., H. Schneider, T. J. Magnani, and S. B. Formal. 1964. Epithelial cell penetration as an essential step in pathogenesis of bacillary dysentery. *J. Bacteriol.* 88:1503–1518.
45. Lin, C.-S., R. Aebersold, and J. Leavitt. 1990. Correction of the N-terminal sequences of the human plastin isoforms by using anchored polymerase chain reaction: identification of a potential calcium-binding domain. *Mol. Cell. Biol.* 10:1818–1821.
46. Lin, C. S., R. H. Aebersold, S. B. Kent, M. Varma, and J. Leavitt. 1988. Molecular cloning and characterization of plastin, a human leukocyte protein expressed in transformed human fibroblasts. *Mol. Cell. Biol.* 8:4659–4668.
47. Majeed, M., and E. Kihlström. 1991. Mobilization of F-actin and clathrin during redistribution of *Chlamydia trachomatis* to an intracellular site in eukaryotic cells. *Infect. Immun.* 59:4465–4472.
48. Makino, S., C. Sasakawa, K. Kamata, T. Kurata, and M. Yoshikawa. 1986. A genetic determinant required for continuous reinfection of adjacent cells on large plasmid in *S. flexneri* 2a. *Cell.* 46:551–555.
49. Matsudaira, P., E. Mandelkow, W. Renner, L. K. Hesterberg, and K. Weber. 1983. Role of fimbrin and villin in determining the interfilament distances of actin bundles. *Nature (Lond.).* 301:209–214.
50. Maurelli, A. T., B. Baudry, H. d'Hauteville, T. L. Hale, and P. J. Sansonetti. 1985. Cloning of plasmid DNA sequences involved in invasion of HeLa cells by *Shigella flexneri. Infect. Immun.* 49:164–171.
51. Menard, R., P. J. Sansonetti, and C. Parsot. 1993. Nonpolar mutagenesis of the *ipa* genes defines IpaB, IpaC, and IpaD as effectors of *Shigella flexneri* entry into epithelial cells. *J. Bacteriol.* 175:5899–5906.
52. Mooseker, M. S. 1985. Organization, chemistry, and assembly of the cytoskeletal apparatus of the intestinal brush border. *Annu. Rev. Cell Biol.* 1:209–241.
53. Mounier, J., T. Vasselon, R. Hellio, M. Lesourd, and P. J. Sansonetti. 1992. *Shigella flexneri* enters human colonic Caco-2 epithelial cells through the basolateral pole. *Infect. Immun.* 60:237–248.
54. Offer, G., C. Moos, and R. Starr. 1973. A new protein of the thick filaments of vertebrate skeletal myofibrils. *J. Mol. Biol.* 74:653–676.
55. Ogawa, H., A. Nakamura, and R. Nakaya. 1968. Cinemicrographic study of tissue cell cultures infected with *Shigella flexneri. JPN J. Med. Sci. Biol.* 21:259–273.
56. Pace, J., M. J. Hayman, and J. E. Galan. 1993. Signal transduction and invasion of epithelial cells by *S. typhimurium. Cell.* 72:505–514.
57. Prévost, M. C., M. Lesourd, M. Arpin, F. Vernel, J. Mounier, R. Hellio, and P. J. Sansonetti. 1992. Unipolar reorganization of F-actin layer at bacterial division and bundling of actin filaments by plastin correlate with movement of *Shigella flexneri* within HeLa cells. *Infect. Immun.* 60: 4088–4099.
58. Reynolds, D. J., and J. H. Pearce. 1991. Endocytic mechanisms utilized by chlamydiae and their influence on induction of productive infection. *Infect. Immun.* 59:3033–3039.
59. Rosenshine, I., and B. B. Finlay. 1993. Exploitation of host signal transduction pathways and cytoskeletal functions by invasive bacteria. *BioEssays.* 15:17–24.
60. Sansonetti, P. J. 1983. Alterations in the pathogenicity of *Escherichia coli* K-12 after transfer of plasmid and chromosomal genes from *Shigella flexneri. Infect. Immun.* 39:1392–1402.
61. Sansonetti, P. J. 1992. Molecular and cellular biology of *Shigella flexneri* invasiveness: from cell assay systems to shigellosis. *Curr. Top. Microbiol. Immunol.* 180:1–19.
62. Sansonetti, P. J., D. J. Kopecko, and S. B. Formal. 1982. Involvement of a plasmid in the invasive ability of *Shigella flexneri. Infect. Immun.* 35:852–860.
63. Sansonetti, P. J., J. Mounier, M. C. Prévost, and R.-M. Mège. 1994. Cadherin expression is required for the spread of *Shigella flexneri* between epithelial cells. *Cell.* 76:829–839.

64. Sansonetti, P. J., A. Ryter, P. Clerc, A. T. Maurelli, and J. Mounier. 1986. Multiplication of *Shigella flexneri* within HeLa cells: lysis of the phagocytic vacuole and plasmid-mediated contact hemolysis. *Infect. Immun.* 51:461–469.
65. Stendahl, O., J. H. Hartwig, E. A. Brotschi, and T. P. Stossel. 1980. Distribution of actin-binding protein and myosin in macrophages during spreading and phagocytosis. *J. Cell Biol.* 84:215–224.
66. Takeuchi, A. 1967. Electron microscope studies of experimental Salmonella infection. I. Penetration into the intestinal epithelium by *Salmonella typhimurium*. *Am. J. Pathol.* 50:109–136.
67. Takeuchi, A., H. Sprinz, E. H. La Brec, and S. B. Formal. 1965. Experimental bacillary dysentery: an electron microscopic study of the response of the intestinal mucosa to bacterial invasion. *Am. J. Pathol.* 47:1011–1044.
68. Tilney, L. G., and D. A. Portnoy. 1989. Actin filaments and the growth, movement, and spread of the intracellular bacterial parasite, *Listeria monocytogenes*. *J. Cell Biol.* 109:1597–1608.
69. Vasselon, T., J. Mounier, M. C. Prevost, R. Hellio, and P. J. Sansonetti. 1991. Stress fiber-based movement of *Shigella flexneri* within cells. *Infect. Immun.* 59:1723–1732.
70. Voino, Yasenetzky, M. V., and T. N. Khaokin. 1964. A study of intraepithelial localization of dysentery causative agents with the aid of fluorescent antibodies. *J. Microbiol.* 12:98–100.
71. Young, V. B., S. Falkow, and G. K. Schoolnik. 1992. The invasin protein of *Yersinia enterocolitica*: internalization of invasin-bearing bacteria by eukaryotic cells is associated with reorganization of the cytoskeleton. *J. Cell Biol.* 116:197–207.